

LA-UR- 08-5651

Approved for public release;
distribution is unlimited.

Title: A stable and efficient numerical algorithm for unconfined aquifer analysis

Author(s): Elizabeth Keating and George Zyvoloski

Intended for: Publication in Groundwater



Los Alamos National Laboratory, an affirmative action/equal opportunity employer, is operated by the Los Alamos National Security, LLC for the National Nuclear Security Administration of the U.S. Department of Energy under contract DE-AC52-06NA25396. By acceptance of this article, the publisher recognizes that the U.S. Government retains a nonexclusive, royalty-free license to publish or reproduce the published form of this contribution, or to allow others to do so, for U.S. Government purposes. Los Alamos National Laboratory requests that the publisher identify this article as work performed under the auspices of the U.S. Department of Energy. Los Alamos National Laboratory strongly supports academic freedom and a researcher's right to publish; as an institution, however, the Laboratory does not endorse the viewpoint of a publication or guarantee its technical correctness.

A STABLE AND EFFICIENT NUMERICAL ALGORITHM FOR UNCONFINED AQUIFER ANALYSIS

Elizabeth Keating and George Zyvoloski

Abstract

The non-linearity of equations governing flow in unconfined aquifers poses challenges for numerical models, particularly in field-scale applications. Existing methods are often unstable, do not converge, or require extremely fine grids and small time steps. Standard modeling procedures such as automated model calibration and Monte Carlo uncertainty analysis typically require thousands of forward model runs. Stable and efficient model performance is essential to these analyses. We propose a new method that offers improvements in stability and efficiency, and is relatively tolerant of coarse grids. It applies a strategy similar to that in the MODFLOW code to solution of Richard's Equation with a grid-dependent pressure/saturation relationship. The method imposes a contrast between horizontal and vertical permeability in gridblocks containing the water table. We establish the accuracy of the method by comparison to an analytical solution for radial flow to a well in an unconfined aquifer with delayed yield. Using a suite of test problems, we demonstrate the efficiencies gained in speed and accuracy over two-phase simulations, and improved stability when compared to MODFLOW. The advantages for applications to transient unconfined aquifer analysis are clearly demonstrated by our examples. We also demonstrate applicability to mixed vadose zone/ saturated zone applications, including transport, and find that the method shows great promise for these types of problem, as well.

Introduction

Efficient and accurate methods for simulating groundwater flow in unconfined aquifers systems are required for many applications. Analytical methods are suitable for specific applications such as pump test analysis (Neuman, 1972, etc.). In shallow aquifers where flow is primarily horizontal, the Dupuit approximation (Freeze and Cherry (1979) and analytic element methods (Strack, 1989) have been used successfully. More general methods available for simulating 3-D flow with arbitrary boundary conditions and aquifer heterogeneity include MODFLOW (Harbaugh et al., 2000), coupled unsaturated/ saturated zone codes (InHM (Vander Kwaak (1999), MIKESHE (MIKESHE, 2008) and multi-phase simulation codes such as TOUGH2 (Preuss, 2004) and FEHM (Zyvoloski, 2007). One important advantage of the MODFLOW code is its ability to effectively approximate the water table location at sub-grid scales. This allows simulation of unconfined aquifer problems at large-scales (kilometers) without requiring prohibitively large numbers of gridblocks. Disadvantages include numerical instability (Naff et al. 2003) and errors when the water table is steep and crosses hydrostratigraphic boundaries. In addition, vadose zone processes cannot be simulated. Other methods, in contrast, offer the advantage of more complete representation of both saturated and unsaturated zone flow physics, yet require very small grid blocks and time steps which are frequently prohibitive in large-scale simulations. The additional computational burden required for simulating

unsaturated flow is rarely justified if saturated, unconfined flow is the primary focus. For example, Neuman (1972) showed that for simulating drawdown in pumped unconfined aquifers, considering unsaturated flow theory is unnecessary. For all of these reasons and others, multi-phase codes are rarely used in site-scale or basin-scale unconfined aquifer analysis. There remains a need, however, to develop new numerical methods which tolerate large gridblocks and time-steps necessary for site- and basin-scale applications, can locate the water table at a sub-grid scale, yet are numerically stable. We first review existing methods.

Perhaps the most widely used method for solving unconfined aquifer problems is that employed by MODFLOW. Depending on whether a gridblock is entirely saturated or contains the water table, this code either solves the confined aquifer flow equation (1) or the unconfined flow equation (2) (we omit sinks and sources for simplicity)

$$Ss \frac{\partial h}{\partial t} = K \nabla^2 h \quad (1)$$

$$S_y \frac{\partial h}{\partial t} = \nabla \cdot (Kb \nabla h) \quad (2)$$

where h = hydraulic head (m), t is time (s), K = hydraulic conductivity (m/s), Ss is specific storage (1/m), b is saturated thickness in a water table cell (m). A grid cell containing the water table is conceptualized as having a saturated thickness b derived from the calculated head in the cell, as shown in Figure 1. Vertical conductivity is either unaffected (BCF package) or varies with saturation (LCF package). If the saturation becomes 0 (dry cell) the cell is changed to “inactive” status which can only be reactivated at a later time under specific set of conditions. The selection of the BCF or the LCF package can have a profound effect on the numerical convergence of a water table problem.

This explicit formulation can be numerically unstable in large problems with many grid cells and large fluctuations (over many gridblocks) in water table elevations. Non-unique solutions can be a problem under some conditions, as well (Banta et al, 2006, Naff et al 2003). These problems are, in part, due to the Picard iteration solution and lack of upwinding of saturation-dependent hydraulic conductivities (Peaceman,1977). Another source of instability is the inherently explicit formulation whereby recharge sources must be always be applied in water table gridblocks and so as the water table moves into new gridblocks the source terms must be moved as well (Harbaugh et al., 2000).

While considerable progress has been made in the control of oscillations (Doherty 2001, Banta 2006), this control is dependent on four input parameters (WETFCT, IHDWET, IWETIT, WETDRY) that are mildly to strongly problem dependent. A frequently used strategy to improve convergence is to design the grid, using sloping layers and/or very thick layers, such that the water table never moves out of a single layer. However, sloping grids introduce errors associated with missing terms in finite difference stencil. Errors associated with these approaches have been discussed in Zyvoloski and Vessilinov (2006).

Numerical methods developed primarily for multiphase flow applications can, in theory, be used to simulate unconfined aquifers as well as vadose zone processes above the water table. Mass conservation equations are expressed for each phase, as follows:

$$\frac{\partial(\theta_m \rho_m \phi)}{\partial t} = \nabla \cdot \left[\frac{k'(\theta_m) k \rho_m}{\mu_m} (\nabla p_m - \rho_m g z) \right] \quad (3)$$

Where the subscript m refers to the phase (air or water). For groundwater flow applications where air and water are the two phases of interest, two simultaneous equations representing the conservation of air and water mass are solved. Air pressure, p_a , and water saturation θ_w are typically the two primary variables. Additional equations defining relatively permeability for each phase, and capillary pressure, $p_c = p_a - p_w$, are also required (Forsyth, 1988). Above the water table a simplifying assumption of constant air pressure can be invoked to reduce the computational burden; this is equivalent to solving Richard's Equation.

Neglecting the air phase and considering only the water balance, the solution of Equation (3) for both unsaturated and saturated flow is still numerically challenging, particularly at the interface between the two flow regimes (the water table). Freeze (1971) developed a formulation that used pressure head ($\psi = p/\rho g$) as the independent variable both above and below the water table. He noted that functional continuity was maintained as the pressure head transitioned from negative values in the unsaturated region to positive values in the saturated zone. Alternative approaches have been developed which employ variable switching (Forsyth et. al, 1995, Kirkham and Hillis (1991, and Huyakorn and Pinder, 1983). In these methods, saturation and pressure are independent variables in the unsaturated and saturated regions respectively. Forsyth et. al, (1995) reported that switching variables between pressure and water content could be more efficient than using a for problems with very dry initial conditions and very high capillary pressures.

Numerical schemes using Newton Raphson iterations are generally more stable and converge faster than those using Picard iterations, but they require continuous derivatives to achieve theoretical (second order) convergence rates. This is problematic near the water table, where there are discontinuities in the derivatives of the saturation – pressure head relationship as well as the storage term. These discontinuities often cause excessive iterations when a gridblock is converting from a partially saturated to a saturated condition (or vice versa); the severity of this problem is strongly dependent on the form of the saturation/pressure relationship for a particular soil.

Strictly speaking, these methods that solve both saturated and unsaturated flow equations can identify the elevation of the water table with accuracy no greater than the vertical dimension of one gridblock. Once a gridblock becomes partially saturated, it experiences relative permeability and capillary pressure effects and water flow is reduced compared to saturated flow. This is not an important limitation for many vadose zone applications, especially those where small vertical grid discretization is possible. This issue will be clearly illustrated in the following sections when we compare mixed unsaturated/saturated flow equations results with our new method.

New formulation

Here we present a new approach which combines features of the coupled unsaturated / saturated flow equation solution methodology first reported by Forsyth (1988) and the approximation to sub-gridblock-scale water table evaluation used in MODFLOW. We use an existing code developed for multiphase flow (FEHM, Zyvoloski, 2007) which solves the numerical analogue of equation (3)

$$V_i \frac{\left[(\theta \rho_w \phi)_i^{n+1} - (\theta \rho_w \phi)_i^n \right]}{\Delta t} - \sum_{\text{neighbor cells}} \left(\frac{k'(\theta) \rho_w}{\mu_w} \right)_{ij} k_{hx} \cdot \left(\frac{A_j}{\Delta d_j} \right) \cdot \left[(p_{wj} - p_{wi}) - (\rho_w g)_{ij} (z_j - z_i) \right] = 0 \quad (5)$$

The summation refers to neighboring nodes, j , connected to node i . Here the $(\cdot)_{ij}$ represents some inter-nodal averaging of the nonlinear part of the hydraulic conductivity term. The term k_{har} refers to the harmonic weighting of the intrinsic permeability if gridblocks i and j . The term V_i is the volume of the gridblock surrounding node i . The area factor $(A_{ij}/\Delta d_{ij})$ refers to the internodal area divided by distance between nodes i and j . Harmonic, arithmetic, and (flow) upwinded internodal evaluation can all be used as internodal averaging of the hydraulic conductivity term. Using the upwinded value facilitates stable and monotonic numerical simulation of multiphase flow (Peaceman, 1978).

Our new approach solves the equation (5), with p_w as the primary variable and assumes constant air pressure. We couple Equation 5 with a linear pressure / saturation relationship customized to represent the water table elevation at the sub-gridblock scale, as illustrated in Figure 1. For a gridblock of thickness Δz , where z ranges from z_1 and z_2 , saturation is calculated during each Newton-Raphson iteration directly from block pressure, or equivalently, of head ($h = \frac{p_w}{\rho g} + z$), as follows:

$$\begin{aligned} \text{If } z_2 < h < z_1, \theta &= \frac{h - z_2}{z_1 - z_2} \\ \text{If } h > z_1, \theta &= 1 \\ \text{If } h < z_2, \theta &= 0 \end{aligned} \quad (6)$$

Furthermore, if the calculated head of a cell falls below the elevation of the bottom of a grid block, the head in the grid block is set to the elevation of the bottom of a grid block ($h=z_1$ or $p_w = -0.5\Delta z$). The resulting pressure / saturation relationship for cells with $h \leq z_1$ is shown in Figure 2. In partially saturated cells, this is very similar to solving Equation 3 with a linear capillary pressure model, except that water pressure is slightly negative in cells with zero saturation. The value of pressure at zero saturation is strictly grid-size dependent and does not represent a physical capillary pressure. As will be shown in the final example problems below, significant numerical advantages are gained by this particular choice of pressure / saturation relationship for both unconfined aquifer problems and coupled unsaturated / saturated flow problems.

In our approach, the permeability in a partially-saturated cell containing the water table is modified in a similar fashion to that employed by MODFLOW. Horizontal permeability is scaled by saturation. The conceptual model (Figure 1) requires that vertical permeability in the partially saturated cell be unaffected by saturation. However, this creates a derivative discontinuity that poses a problem for convergence and stability. To address this problem, we employ a user-specified parameter A , typically $1 < A < 1000$, which is the ratio of the vertical to horizontal permeability scaling factor. The higher the value of A , the stronger the hydraulic connection between the cell containing the water table and the cell below it and therefore the more faithful the formulation is to our conceptual model (Figure 1). The resulting equations are as follows:

$$\begin{aligned} k'_{xy}(\theta) &= \theta \\ k'_{z} &= \min(1, A \theta) \end{aligned} \quad (7)$$

The importance of the parameter A increases as with the height of the grid block. As will be shown below, a value of ten works well for most problems.

The Newton-Raphson method is well suited to water table problems because of the implicit accounting at each iteration of the nonlinear terms. It is much less prone to the oscillatory behavior of the Picard iteration process. The Newton-Raphson method requires only one parameter: the solution tolerance. We explored both arithmetic and upwinded weighting of the interblock hydraulic conductivity term. For all but the easiest problems, upwinding this term was required for convergence. We use a preconditioned Krylov space solver with incomplete factorization as the preconditioner (see Zyvoloski (1986), Van der Vorst (1992)).

The result is a formulation that does not require dry cells to become inactive; rather, they can continue to conduct flow according to Richard's Equation coupled with a linear pressure/ saturation relationship (Equation 5). A very advantageous consequence of this is that recharge sources can be placed statically in realistic locations, such as ground surface, rather than artificially moved down to water table cells, such as is required in MODFLOW. Our formulation uses a single variable, p_w , for both unsaturated and saturated conditions. We present three examples to illustrate the accuracy of the formulation, its sensitivity to grid block size, and its efficiency. In the first example, we demonstrate the accuracy of our methodology by comparison to an analytical solution (Neuman, 1972) for radial flow to a well in an unconfined aquifer. Using this example, we also demonstrate the gains in computational efficiency and numerical accuracy by comparison to a two-phase (air/water) flow calculation, the methodology employed for the two-phase approach has been benchmarked against a variety of validation problems (Forsyth et al. 1995, Forsyth, 1988). For this and all the following examples, the two-phase simulations assume a simple linear relative model with no residual saturation and zero capillary pressure at all saturations. This corresponds to the conceptual model of a water table unaffected by capillary forces, as would be the case in coarse-grained aquifers.

We also demonstrate advantages in stability by comparison to a solution of the unconfined pumping using MODFLOW. In the second example, we show a 3-D simulation of a simple unconfined aquifer stressed by alternating high and low recharge rates resulting in large fluctuations in water table elevation. Using a high-resolution 2-phase simulation as the benchmark, we examine the accuracy and numerical efficiency of our formulation during the water table rise and fall cycles and explore the influence of grid size. Finally, we present a simulation of flow and transport through the vadose zone into an unconfined aquifer. This comparison illustrates the potential utility of this formulation for unsaturated flow, despite the inherent contradiction between our conceptual model (Figure 1), intended to replicate a continuously saturated water column, and vadose zone flow.

In all example problems, the water table location was calculated by analyzing the water content in each vertical column of gridblocks as follows. For each column of gridblocks, the lowest elevation partially saturated gridblock was identified. The head calculated in this gridblock was used to define the water table elevation partially saturated grid block immediately above was taken to represent the water table elevation, as shown in Figure 1.

Radial flow to a well in an unconfined aquifer

Neuman (1972) presented an analytical solution to radial flow and drawdown during pumping in an unconfined aquifer. His solution highlights three phases during drawdown, early times when water is primarily released from elastic storage, intermediate times when water continues to be released from storage but also pore drainage occurs at the water table, and late times when pore

drainage is the dominant mechanism. His expression calculates drawdown ($dh(x,y)$) as a function of pumping rate (Q), aquifer thickness (D), Specific storage (S_s), Specific yield (S_y), Hydraulic conductivity (K_x), and the ratio of vertical to horizontal conductivity (K_x/K_y).

For parameters listed in Table 1, we developed a radial flow model shown in Figure 3. A pumping well is at $r=0$. The analytical solution is shown in Figure 4. For comparison, a Theis solution and a “instantaneous drainage” solution are also shown. We compare this analytical solution with the solution from our new single phase algorithm and an exact two-phase (air/water) solution for four grid with varying resolutions in the z direction. The single phase method agrees very well with the analytical solution for all four grid resolutions. There are small discrepancies at very early times. The two-phase provides a less accurate solution even at the finest grid resolution, and requires an order of magnitude more computational effort (see Table 2). At the coarsest grid resolution, the early time drawdown is particularly problematic. The relatively poor performance of the two-phase model is worth consideration. In the absence of capillary forces, the two-phase model will only be able to resolve the water table to within one grid block. This induces a granularity to the solution of a moving water table problem that compromises the accuracy of this method for this type of application.

Comparison with MODFLOW

Using the same model application, we compare our method to that employed by MODFLOW Version 1.15 (Harbaugh et al. 2000). Aquifer parameters (S_s , S_y , and permeability, Table 1) were converted to MODFLOW units and specified accordingly. To ease the numerical comparison, we place the pumping well in the center of a symmetric 3-D grid, 125.4 m by 125.4 m by 10 m. Grid spacing expands geometrically from a minimum of 0.5 m in the x and y directions at the center of the grid, where the pumping occurs, to a maximum of 4.2 m at lateral boundary. A uniform grid spacing in the vertical direction of 1m was used. Grids for FEHM and MODFLOW were identical. Lateral boundaries are specified head. Pumping was simulated in the bottom 6 layers at a total rate 0.5 kg/s (evenly distributed among the layers) for 100 days followed by a recovery period of 100 days. Variable-length timesteps were used in both pumping and recovery periods, geometrically increasing from an initial step of 5.2 seconds (this is FEHM only, right?). For the MODFLOW simulations, we used the BCF package, which maintains a constant vertical hydraulic conductivity in cells containing the water table. The WETDRY parameter was set to -0.1 For the FEHM simulations, a value of 10 was set for parameter A (Equation 7).

Simulated heads at $x=3.57$, $y=3.57$, $z=4.5$ (the well is at $x=y=0.25$ m) are presented in Figure 5. There is excellent agreement between FEHM and MODFLOW results. There were, however, significant differences in performance, as summarized in Figure 6. The MODFLOW simulations required more iterations per time step during the drawdown phase. MODFLOW required up to 22 iterations per time step, significantly more during drawdown than during recovery. FEHM only required 2-3 (or 1?), and had fairly similar requirements during drawdown and recovery. The lower number of iterations did not, however, result in lower total CPU run times. This is partially due to upwinding, which produces an asymmetric system of algebraic equations requiring more CPU time per iteration to solve. In contrast, MODFLOW utilizes arithmetic or harmonic averaging (Pohll, 2006) and a Picard-type iteration. The net effect was that the total simulation CPU times for the two codes were very similar (within 1-5%).

The instability of the Picard iteration methodology is evident in the oscillatory behavior during drawdown, shown in Figure 6a. This worsened when the pumping rate was increased from 0.5 kg/s to

0.8 kg/s. The MODFLOW simulation failed to converge 40 days into the simulation, despite allowing up to 200 iterations per time step. FEHM was able to converge at this higher pumping rate with the same number of timesteps and a low number of iterations per time step. This is noteworthy since, as shown in Figure 6b, the number of cells converting from saturated to partially saturated was roughly double in the higher pumping rate scenario. In addition to the obvious consequences of non-convergence, the determination and control of numerical truncation errors associated with grid size would be impossible for the MODFLOW simulations in this case.

3-D flow with transient recharge (wetting and drying)

This example is intended to test the performance of the algorithm in a 3-D flow problem with transient recharge. The dimension of the problem is 10000 by 10000 by 1000 m, as shown in Figure 8. A line of constant-head nodes is placed at an elevation of 900m, extending from $x = 5000 - 10000$ m at $y = 5000$ m. The initial condition is uniform head = 900 m (flat water table). Permeability is uniform, 10^{-12} m², porosity is 0.25, and there is no elastic storage. At the start of the simulation, 2100 kg/s recharge is applied uniformly across the top of the model for 5000 days. To test sensitivity to grid resolution, we developed three grids, described in Table 4.

Changes in the calculated elevation of the water table as a function of time are shown in Figure 9, comparing the single-phase and two-phase solutions, at three different grid resolutions. For the two finest grids (A and B), the two solution methods are comparable, although the single-phase solution is much smoother. The granularity in the two-phase solution (with zero capillary pressure) is due, at least in part, to the fact that the water pressure in a gridblock is constrained to be at atmospheric pressure until the gridblock is fully saturated. This means there will be no lateral water flow between two partially saturated grid blocks. In contrast, the single-phase formulation allows water to flow from the gridblock with high saturation (and higher pressure) to the gridblock with lower saturation. It is evident in Figure 9. The single-phase solution degrades somewhat at the coarsest grid resolution (errors up to 1-2m); and the two-phase solution has very significant errors (up to 20m).

In Figure 10 we show cross-sections of the water table at time=5000 days (maximum water table elevation) at two values of x . Here we see large differences in the smoothness of the water table. In Table 3 we compare numerical performance of the two methods. In the two finer grids (A and B), the single-phase solution is approximately twice as efficient. Efficiency is comparable in the coarsest grid, but the accuracy of the two-phase solution was very poor.

Extension to mixed vadose / saturated zone simulations

Finally, we test this formulation in a mixed vadose / saturated zone flow and transport application. In this two dimensional example problem we simulate recharge through a heterogeneous vadose zone, including a perching aquitard, into an unconfined aquifer. Like the previous example, this example test the ability of our algorithm to efficiently “flow” water through relatively dry gridblocks which separate the recharge source area and the water table. It also tests the ability of this formulation to simulate perched aquifers which are quite difficult to simulate with MODFLOW (Naff et al. 2003).

Initial conditions consisted of a water table at 600m height in hydrostatic equilibrium. A water table caused by recharge (total inflow = 0.5 kg/s) and inflow and outflow on the side boundaries was

simulated with an increasing time step size until a new steady-state was reached, defined by differences in inflow and outflow rates less than 1.E-3 kg/s. To consider the impact of grid resolution, three different grids were used.(Table 5).

Simulated steady-state saturations for single and two-phase formulations, using the finest grid, are presented in Figures 11 and 12. The total water table change varies from +200m to -500m - depending on the location relative to the source and model boundaries. The water table configuration is similar in both models. The two-phase model, however, shows significant granularity in the water table surface for reasons explained above.

The numerical efficiency of the methods is also summarized in Table 6. The performance of the single-phase method is impressive with a total-run time reduction factor of approximately 3 for the coarse grid and approximately 30 for the finest grid. While part of the improved performance can be attributed to the fact that the two-phase solution solves for two variables while the single-phase algorithm solves for only one, the smoothness of the formulation, as evidenced by the lower iteration count is also a significant factor.

Our final comparison is a simulation of transport of a conservative solute from the recharge source to several observation points in the unconfined aquifer. In this application, we solve the advection-dispersion equation (Freeze (1979)). A solute is released for the first 730 days of the simulation. A value of 1 m for longitudinal and transverse dispersion, no diffusion, and a value of 0.1 for porosity were used. We use the fine grid (Table 5) for the comparison.

We calculated breakthrough curves computed at two locations, shown in Figure 11. Results are presented in Figures 13 and 14. For the shallow observation point at the water table, the two-phase and single phase formulations give nearly identical results. At the deeper observation point near the aquifer outlet, the strongly bi-model breakthrough curves simulated by both methods are nearly identical. This comparison demonstrates the potential utility of this single-phase approach for not only flow but also transport simulations.

Discussion and conclusions

We have presented an efficient, stable method to simulate transient flow in unconfined aquifers. The key part of the formulation is the identification of a saturation-pressure relationship that relates the saturation in a gridblock to the water level in the gridblock relative to the gridblock length in the direction of gravity. Flowing area in the horizontal direction is proportional to saturation. It is equivalent to solving Richard's Equation with a particular, grid-dependent linear relation between pressure and saturation and, as such, can be used to simulate both unsaturated and saturated flow. It is similar conceptually to the method used in the widely available MODFLOW code for unconfined groundwater simulations. The strong vertical coupling in the MODFLOW method is obtained by introducing anisotropic relative permeabilities with the vertical relative permeability assigned a value typically 10 times the horizontal relative permeability. In this sense, our formulation replicates some features of BCF package in MODFLOW. The method is more stable than the MODFLOW formulation and much more numerically efficient than two-phase simulations. The enhanced stability over the MODFLOW formulation is due to the inherent stability of Newton-Raphson iteration scheme the elimination of the requirement to "convert" cells from wet to dry and vice-versa, and the elimination of the need to move recharge sources as the water table moves. One on the consequences of the Newton-Raphson iteration in our formulation is the lack of problem-dependent parameters. The formulation here has one parameter, the vertical conductivity multiplier " A ".

Unlike two-phase simulation methods, the ability to estimate the water table elevation is not strongly dependent on vertical grid spacing and so can be used for practical, field-scale applications. Unlike Richard's Equation coupled to a general pressure / saturation relationship, the pressure at zero saturation is strictly grid-size dependent. This offers significant numerical advantages over more general approaches, but limits its applicability to vadose zone problems with general capillary pressure relationships.

In the examples presented above we have shown the validity of this formulation, compared to an analytical solution (Neuman, 1972), and have demonstrated significant advantages in both accuracy and efficiency over a two-phase formulation. We have also demonstrated enhanced stability when compared to the MODFLOW approach; this is due to several factors, most notably a fully implicit numerical scheme that utilizes upwinding. There is a modest additional CPU requirement, which is likely a consequence of unstructured connectivity. While the grid in this application is clearly orthogonal, we are paying a price for the indirect addressing associated with finite element methods) used in the FEHM code. This disadvantage, while minor, could be eliminated if the method was implemented in a structured-grid code like MODFLOW. We expect that this new method is much more efficient than solving Richard's Equation with a general capillary pressure / saturation relationship, without variable switching, since in the latter case continuous pressure/saturation derivatives would not be guaranteed at the transition between a partially saturated and fully saturated cell. Using FEHM, we have compared it to a variable-switching scheme for solving Richard's Equation with an equivalent capillary pressure / saturation relationship and found it to be equal to or more efficient.

Despite the grid-dependent pressure / saturation relationship, it provides a reasonable approximation to vadose zone pressures, saturations, and consequent solute transport, as demonstrated by comparison with 2-phase simulations. For more general mixed vadose zone / saturated zone applications, errors would have to be evaluated on a case-by-case basis and would be largely dependent on the departure of the "true" saturation / pressure relationship measured in the porous medium from the linear saturation / pressure relationship inherent this method. If departures were large, a more general capillary pressure model would be required and numerical performance would presumably decline.

Ongoing research efforts to couple models developed using FEHM and MODFLOW such as Dickenson et al. (2007) should benefit from the similarity of the water table formulations in the two codes.

Acknowledgements

We thank John Doherty for assisting with MODFLOW runs and for many helpful discussions. We appreciate funding from Los Alamos National Laboratory LDRD program and from the Groundwater Protection Programs. We also thank Zhiming Lu for providing analytical solutions from Neuman (1972).

References

Aziz, K., and T. Settari, Petroleum Reservoir Simulation, Applied Science Publishers, London, 1979

Banta E., Modifications to MODFLOW Boundary Conditions and an Adaptive-Damping Scheme for Picard Iterations for a Highly Nonlinear Regional Model, MODFLOW and More 2006, May 21-24 2006, Golden Colorado.

Doherty, J., 2001, Improved calculations for dewatered cells in MODFLOW, *Ground Water*, 39(6), 863-869.

Dake, L. P., 1978, *Fundamentals of Reservoir Engineering*, Elsevier, New York.

Faunt, C. C., J. B. Blahey, M. C. Hill, F. A D'Agne, and G. A. O'Brien, 2004, Transient numerical model of ground-water flow. In *Evaluation of the Death Valley regional ground-water flow system (DVRFS)*, Nevada and California, W. Belcher, ed.: U.S Geological Survey Scientific Investigations Report 2004-5205, 352p.

Naff, R., Banta E., and J. McCord, Obtaining a Steady State Solution with Elliptic and Parabolic Groundwater Flow Equations under Dewatering Conditions: Experiences with a Basin Model, MODFLOW and More 2003, September 16-19 2003, Golden Colorado.

Pohll, G. M., Niswonger, R. G., Prudic D.E., A New Algorithm to Simulate Free Surface Conditions within MODFLOW, MODFLOW and More 2006, May 21-24 2006, Golden Colorado.

Forsyth, P. A., 1988, Comparison of the single phase and two phase model formulation for saturated-unsaturated groundwater flow, *Comput. Methods Appl. Mech. Engrg.*, 69, pp 243-259.

Forsyth, P. A., Wu, Y.S., and K. Pruess, 1995, Robust numerical methods for saturated-unsaturated flow with dry initial conditions in heterogeneous media, *Advances in Water Resources*, 18, pp 25-38.

Freeze, R.A., Three dimensional transient, saturated-unsaturated flow in a groundwater basin, *Water Resour. Res.* 7 (1971) 347-366.

Freeze, R. A., and J. Cherry, 1979, *Groundwater*, 1978

Harbaugh, A.W., E.R. Banta, M.C. Hill, and M.G. McDonald, 2000, MODFLOW 2000, The U.S. Geological modular ground-water model—User guide to modularization concepts and the ground-water flow process, U.S. Geological Survey Open-File Report 90-392.

Huyakorn, P. S., and G.F. Pinder, 1983, "Computational Methods in Subsurface Flow", Academic Press, NY

McDonald, M. G., and Harbaugh, A.W., 1984, A modular three-dimensional finite-difference ground-water flow model: U. S. Geological Survey Open-File Report 83-875, 528 p.

Neuman, S. P., 1973, Saturated-Usaturated Seepage by Finite Elements, "Journal of the Hydraulics Division", ASCE, VOL 99, No HY12, 2223-2249.

Preuss, K., 2004, Numerical simulation of CO₂ leakage from a geologic disposal reservoir, including transitions from super- to subcritical conditions and boiling of liquid CO₂. *SPE Journal*, June 2004:237-248.

Strack, O.D.L., 1989, "Groundwater Mechanics", Prentice Hall, New Jersey.

Van der Vorst, H.A., 1992, Bi-CGSTAB: A fast and smoothly converging variant of Bi-CG for the solution of nonsymmetric linear systems, *SIAM J. Sci. Statist. Comput.*, 13, 631-644.

Zyvoloski George A, V V Vesselino, 2006, "An Investigation of Numerical Grid Effects in Parameter Estimation" *Ground Water* 44 (6), 814-825. doi:10.1111/j.1745-6584.2006.00203.x

Zyvoloski, G., 1986, Incomplete factorization for finite element methods, *Int. J. Num. Meth. Eng.*, 23, 1101-1109.

Zyvoloski, G. A., Robinson, B. A., Dash, Z. V. and Trease, L. L. 1999. Models and Methods Summary for the FEHMN Application. Document ID: FEHM MMS SC-194, Revision 1.

Zyvoloski, G. A., E. M. Kwicklis, A. A. Eddebbagh, B. W. Arnold, C. C Faunt, and B. A. Robinson, 2003, The site-scale saturated zone flow model for Yucca Mountain: Calibration of different conceptual models and their impact on flow paths. *J. Cont. Hydrol.*, 6263, 731–750.

List of figures

- Figure 1. Two grid blocks. The lower is fully saturated; the upper contains the water table.
- Figure 2. Pressure / saturation relationship
- Figure 3. Computational mesh (grid B, table 1) for radial flow problem and water table configuration at time = 0 and 50 days. Well location and observation point indicated by white figures.
- Figure 4. Results of unconfined pumping problem for four grids, comparing single phase and b) two phase
- Figure 5. MODFLOW , FEHM, Neuman comparison
- Figure 6. Number of dry or partially saturated cells
- Figure 7. Number of iterations per time step
- Figure 8. Computational mesh for 3-D problem, need to show location of x-sections for figure 6 & boundary conditions (need to replace this with better figure)
- Figure 9. Water level elevation changes with time (need to define “water table elevation”
In a UZ problem)
- Figure 10. Water level elevation at time=2500 days along cross-sections indicated in Figure 8.
- Figure 11. Results for mixed vadose / saturated zone simulation using single-phase formulation
- Figure 12. Results for mixed vadose / saturated zone simulation using two-phase formulation

List of tables

- Table 1. Parameters used in Neuman problem
- Table 2. Grid characteristics and numerical performance for Neuman problem
- Table 3. Grid characteristics and numerical performance for 3-D transient recharge problem.
- Table 4. Aquifer Permeability ($\log_{10} m^2$) for perched aquifer problem
- Table 5. Grids used for perched aquifer problem
- Table 6. Numerical performance of mixed vadose/saturated flow problem.

Table 1. Parameters used in Neuman problem

Ss (m-1)	2.86E-3
Sy	.25
Intrinsic perm (log10 m ²)	-11
Pumping rate (kg/s)	2
x	10.3
y	5

Table 2. Grid characteristics and numerical performance for Neuman problem

	A	B	C	D
Dz (z>700)	.01	.1	.5	1
Dz (z<700)	1	.1	.5	1
Total nodes	23408	7676	1596	836
Two-phase				
N-R iterations	39630	4292	919	381
Solver iterations	347865	59353	12810	4058
Time (second)	9341	321	14	5
Single-phase				
N-R iterations	1021	198	185	169
Solver iterations	8040	1971	1480	872
Time	105	8	2	1

Table 3. Grid characteristics and numerical performance for 3-D transient recharge problem.

	A	B	C			
Dx,dy	500	500	500			
Dz, z<800	50	50	50			
Dz, z>800	5	10	50			
	Single-phase			Two-phase		
	A	B	C	A	B	C
N-R /solver/code time						
Rising	188/1225/40	160/930/22	122/572/8	2026/26733/1168	942/13728/352	458/7781
Falling	349/2719/78	161/1192/23	123/695/8	1051/14215/614	600/9004/229	176/250
Total	537/3944/118	321/2122/45	225/1267/16	3077/40948/1782	1542/22732/582	634/1028

Table 4. Aquifer Permeability (log10 m²) for perched aquifer problem

Layer number	1	2	3	4
Log permeability	-11	-15	-14	-13

Table 5. Grid resolution for perched aquifer problem

Model resolution	Coarse	Medium	Fine
(delx,delz) m	(200,200)	(200,50)	(25,25)
Number of gridblocks	520	2080	32000

Table 6. Numerical performance of mixed vadose/saturated flow problem.

	Discharge (kg/s)	Total water mass (kg)*1.E8	NR iter	solver iter	CPU
2-phase					
coarse	.536	7.95	277	3211	1
medium	.534	7.41	671	7728	7
fine	.535	7.34	2469	113744	1741
Single-phase					
coarse	.541	7.13	95	474	0.4
medium	.539	7.16	113	894	2
fine	.534	7.22	268	7229	55

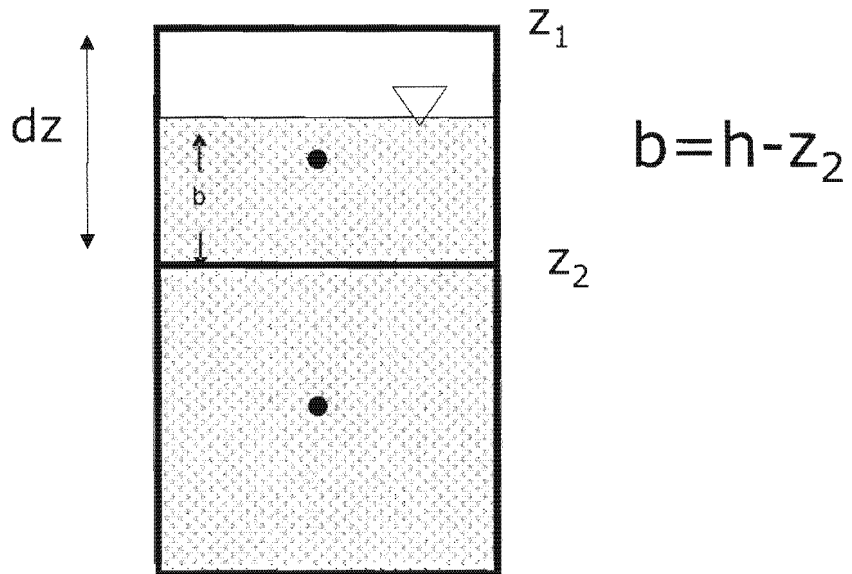


Figure 1. Two grid blocks. The lower is fully saturated; the upper contains the water table. z_1 and z_2 are the upper and lower elevations of the upper cell block. b is the saturated thickness.

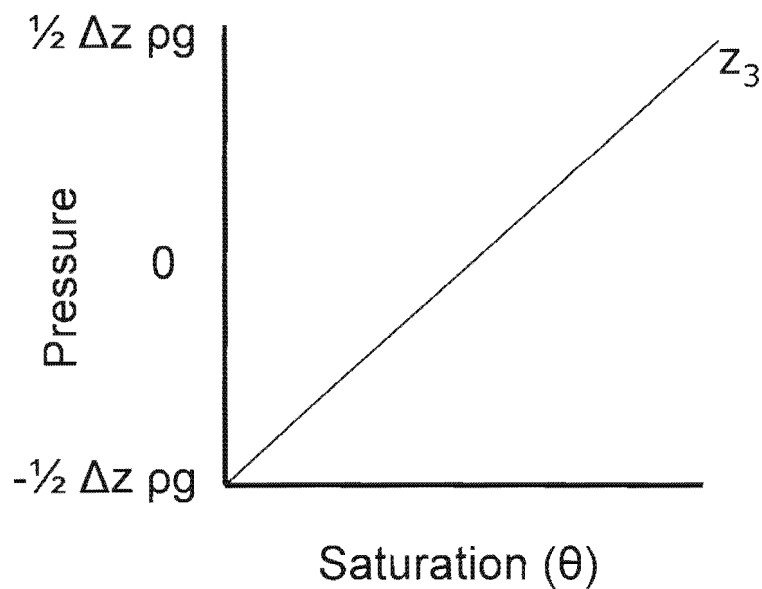


Figure 2. Pressure / saturation relationship in a cell with head $\leq z_1$. Saturation is a dependent variable.

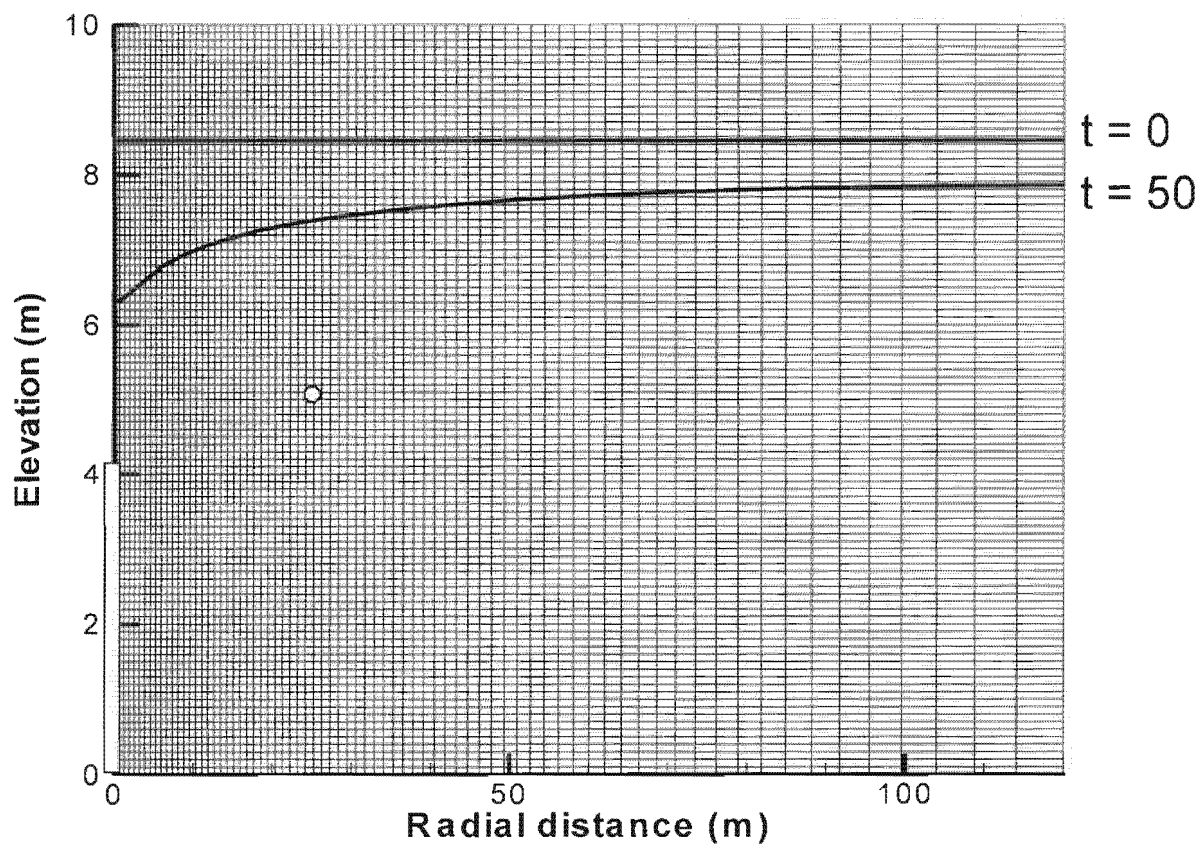


Figure 3. Computational mesh (grid B, table 1) for radial flow problem and water table configuration at time = 0 and 50 days. Well location and observation point indicated by white figures.

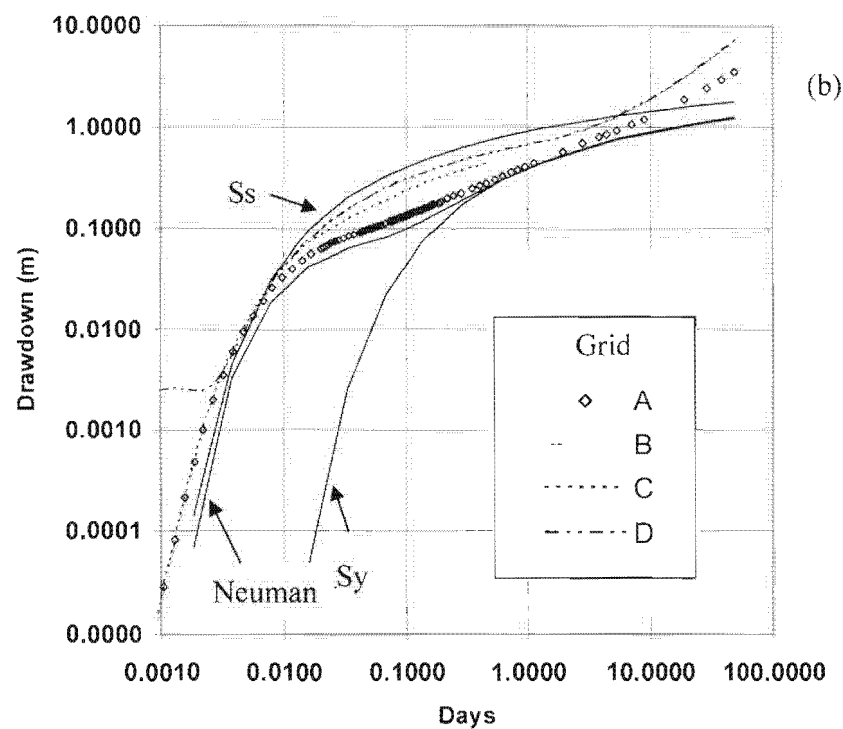
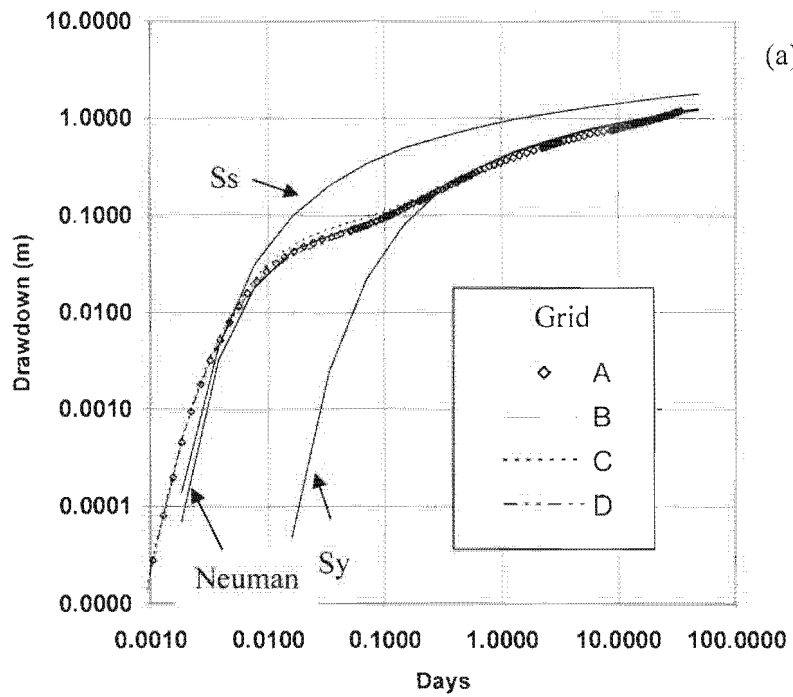


Figure 4. Results of unconfined pumping problem for four grids, comparing
 a) single phase and b) two phase. Solid lines are analytical solutions, Theis (Ss and
 Sy) and Neuman (1972)

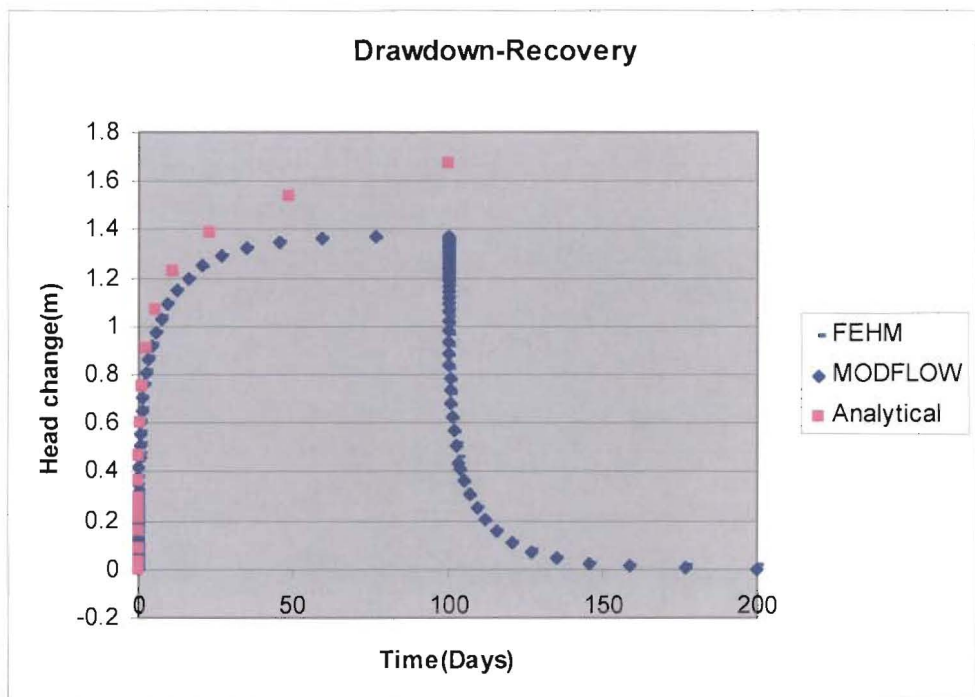


Figure 5. Comparison of FEHM and MODFLOW simulated drawdown and recovery. Analytical solution for drawdown portion

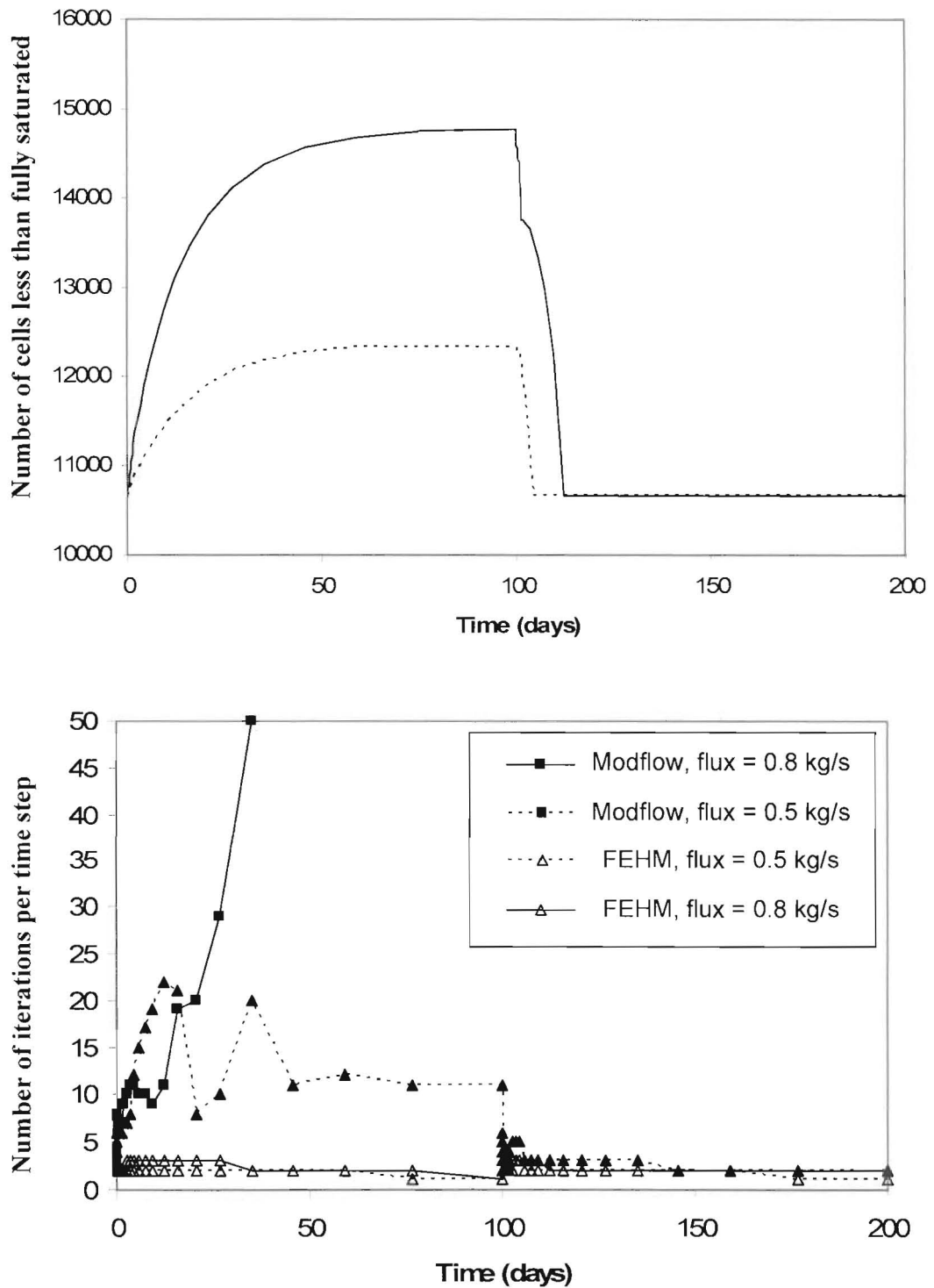


Figure 6a. Number of N-R iterations per time step

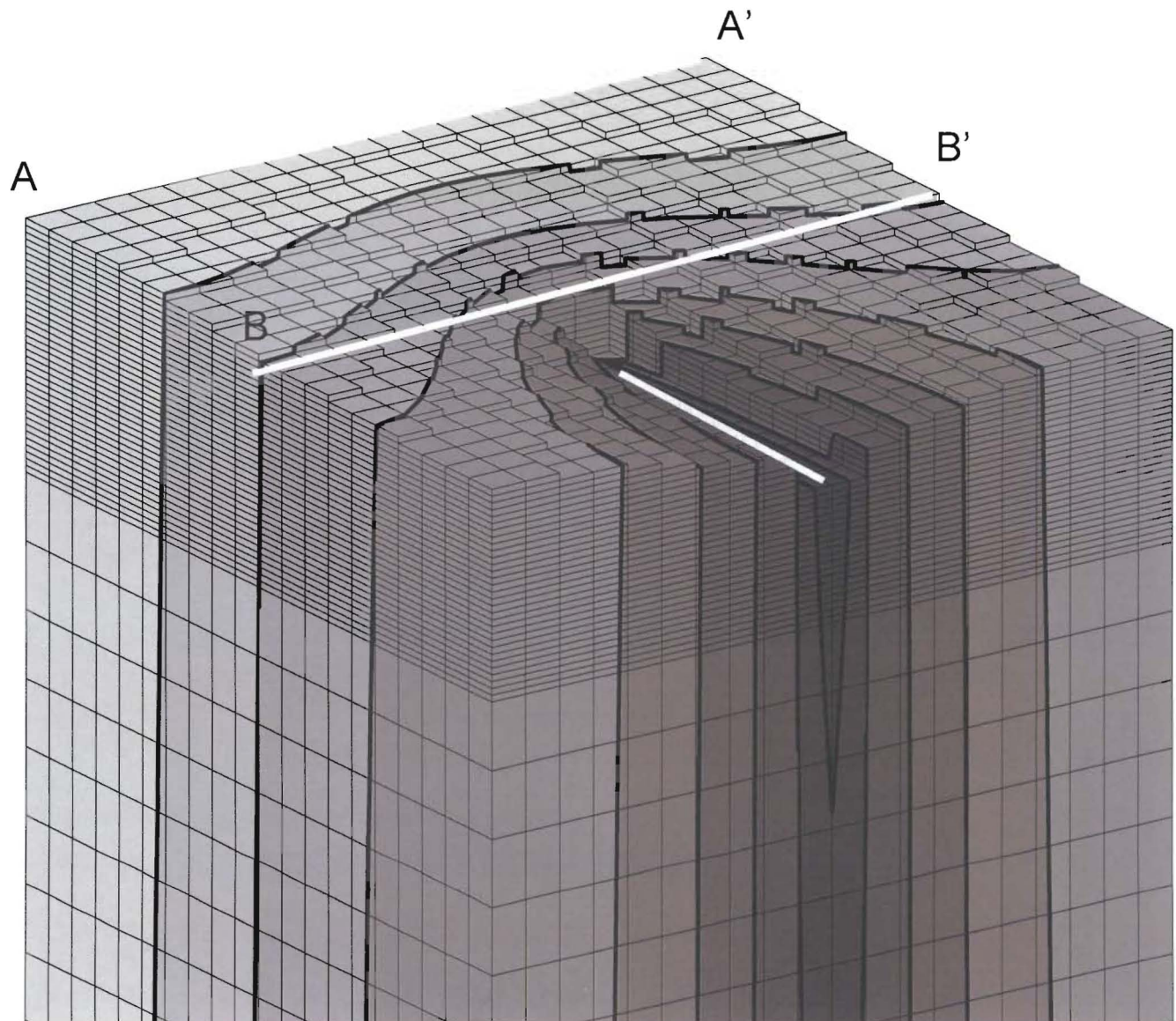
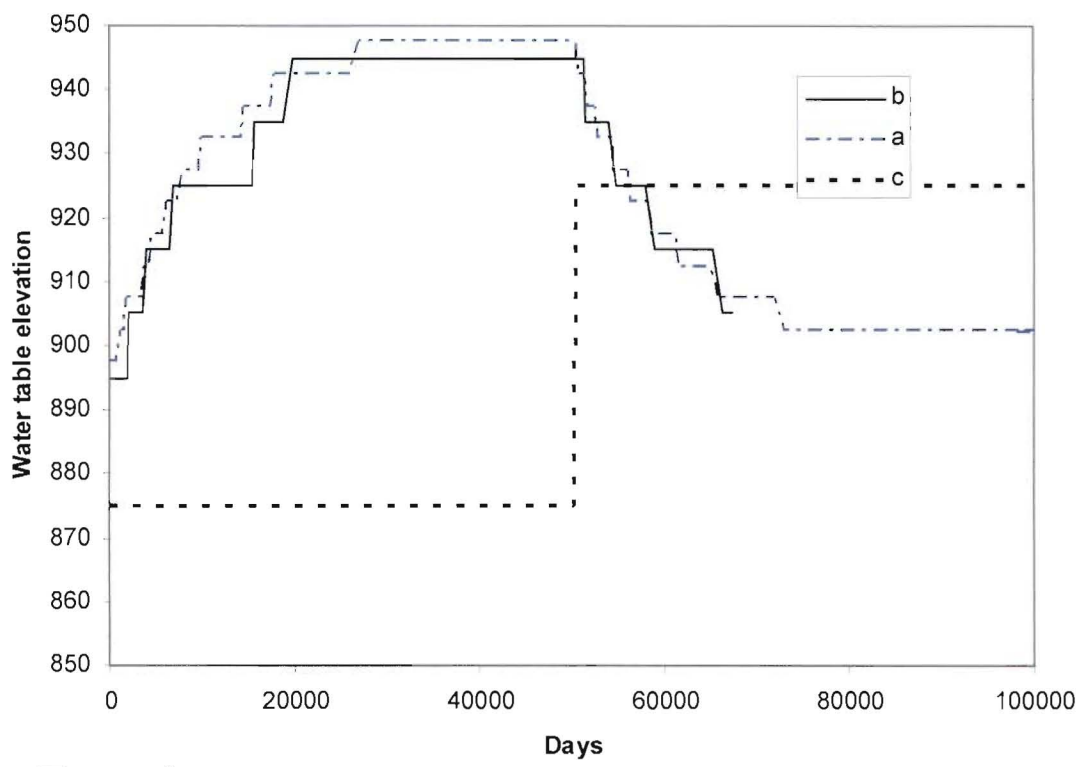


Figure 8. Computational mesh for 3-D problem, showing saturated thickness at time = 44781 days. Dark black lines are head contours at 10 meter intervals. White line shows location of constant head nodes.



Two-phase

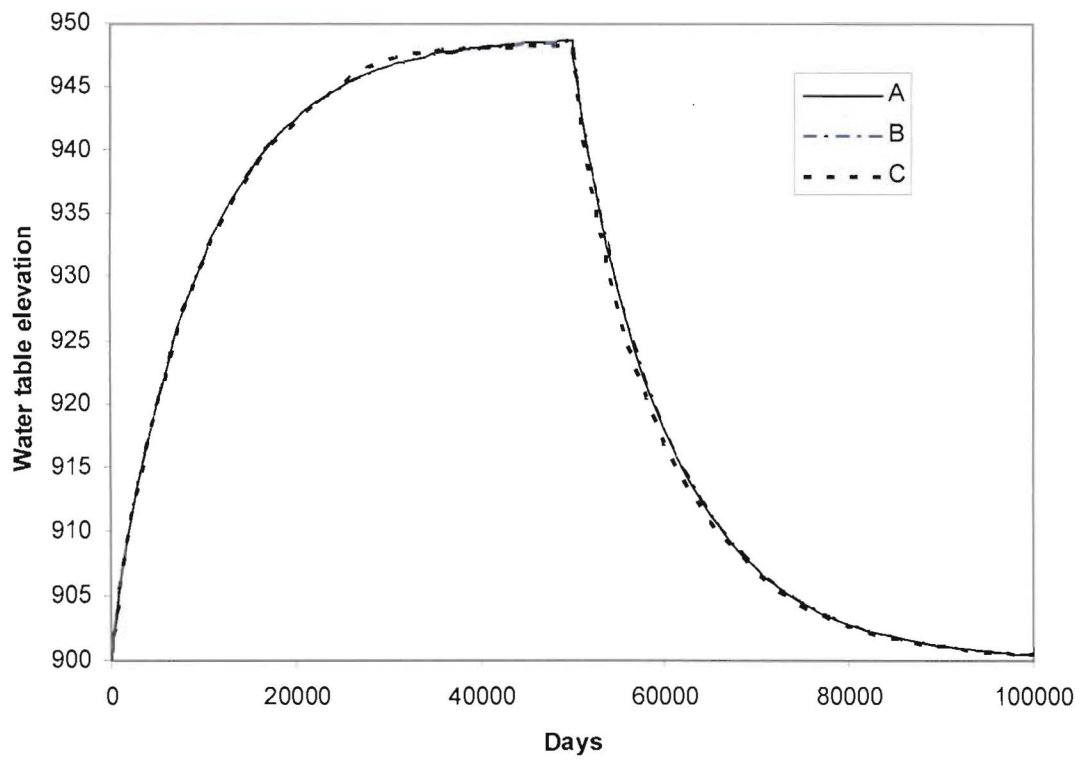


Figure 9. Water level elevation changes with time

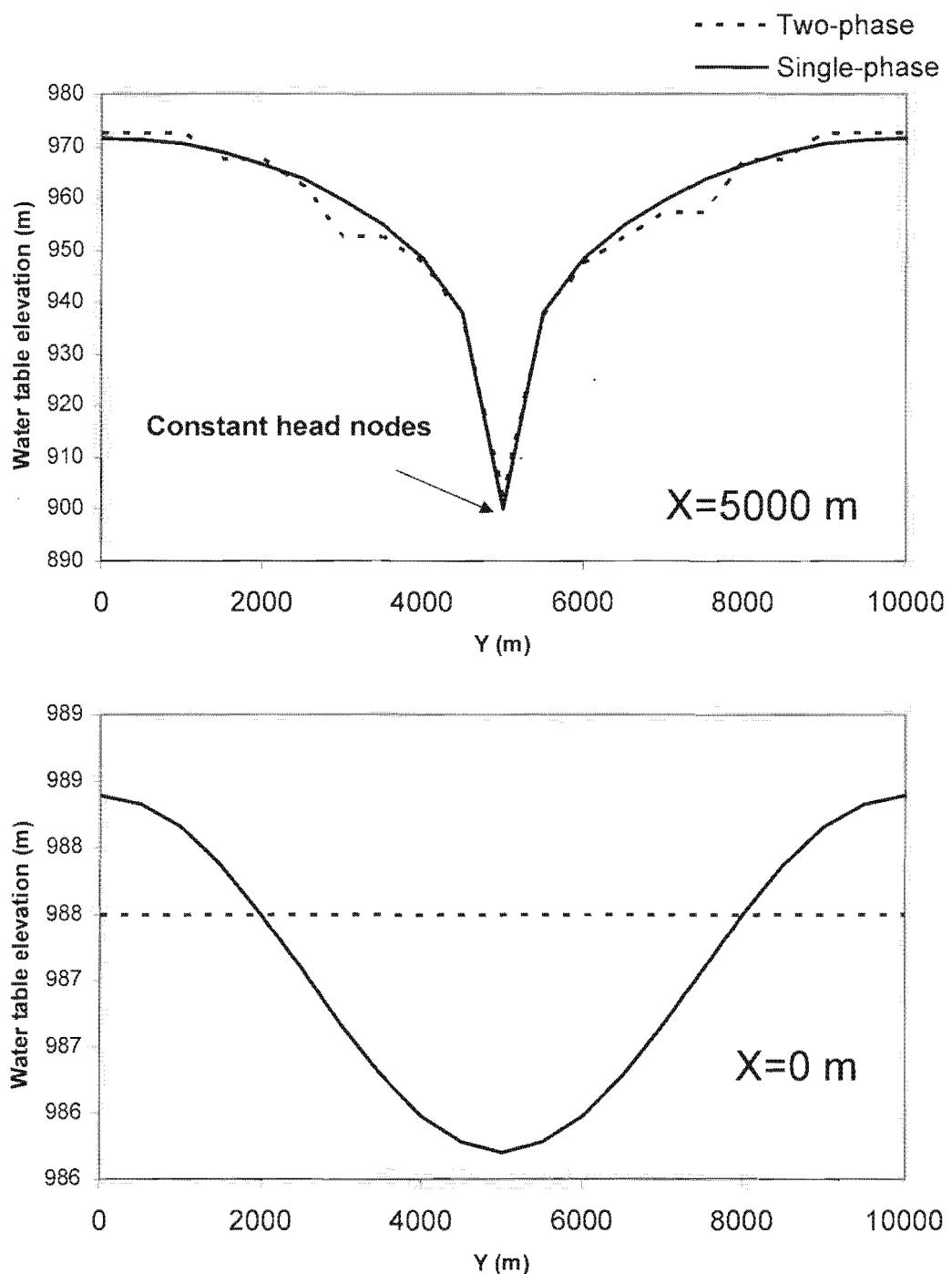
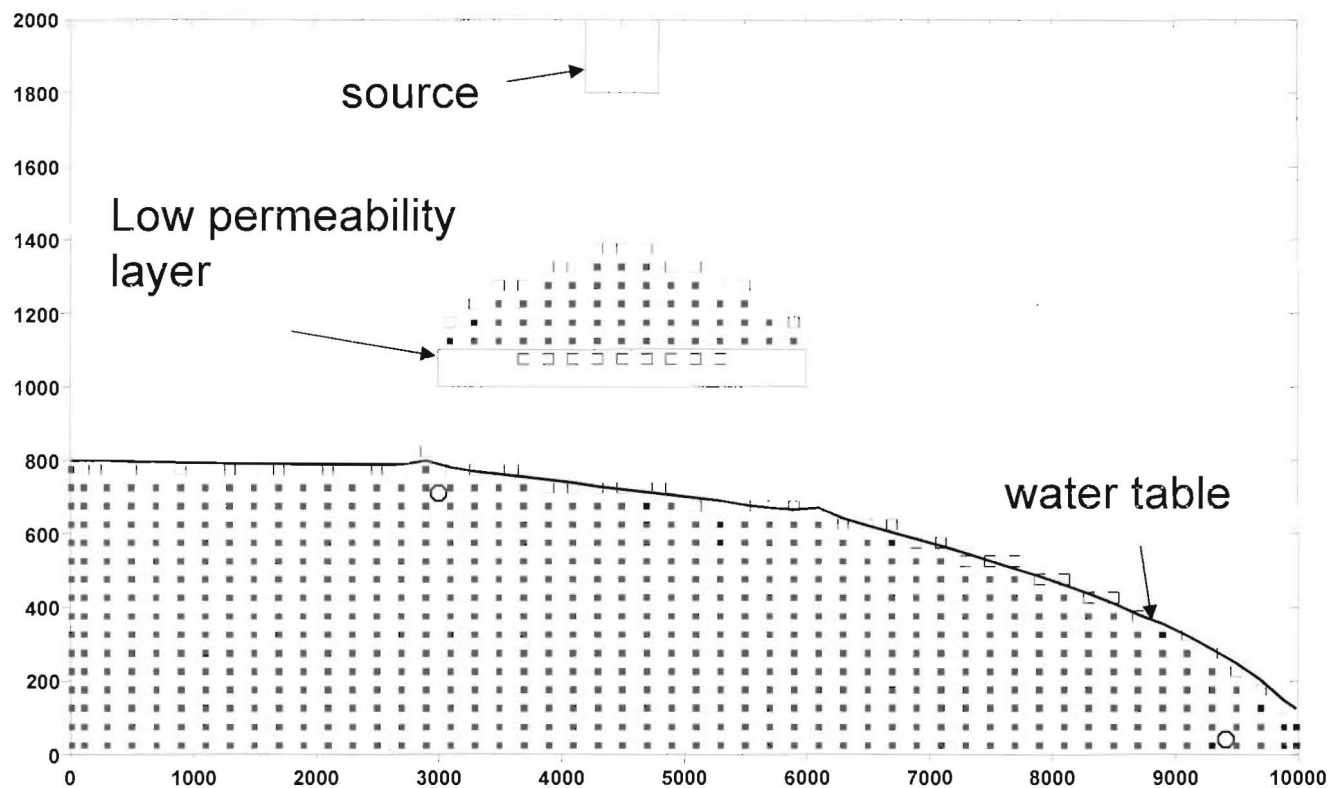
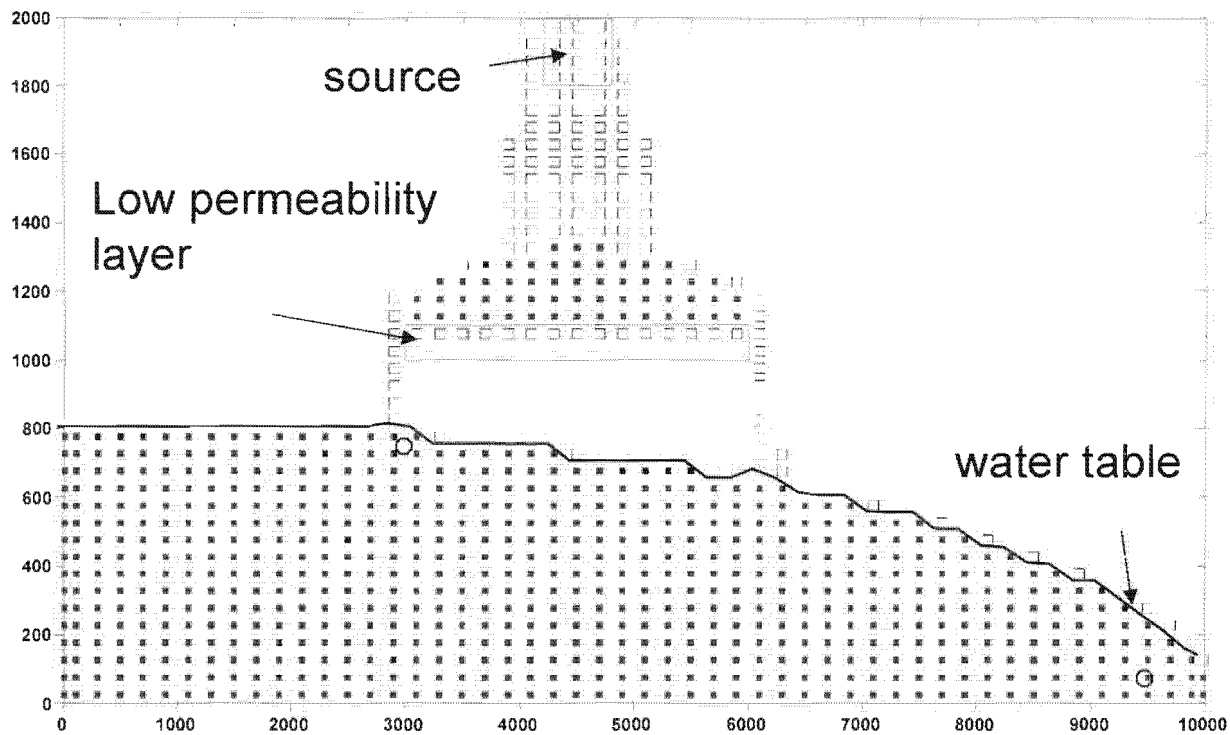


Figure 10. Water level elevation at time=2500 days along cross-sections indicated in Figure 8.



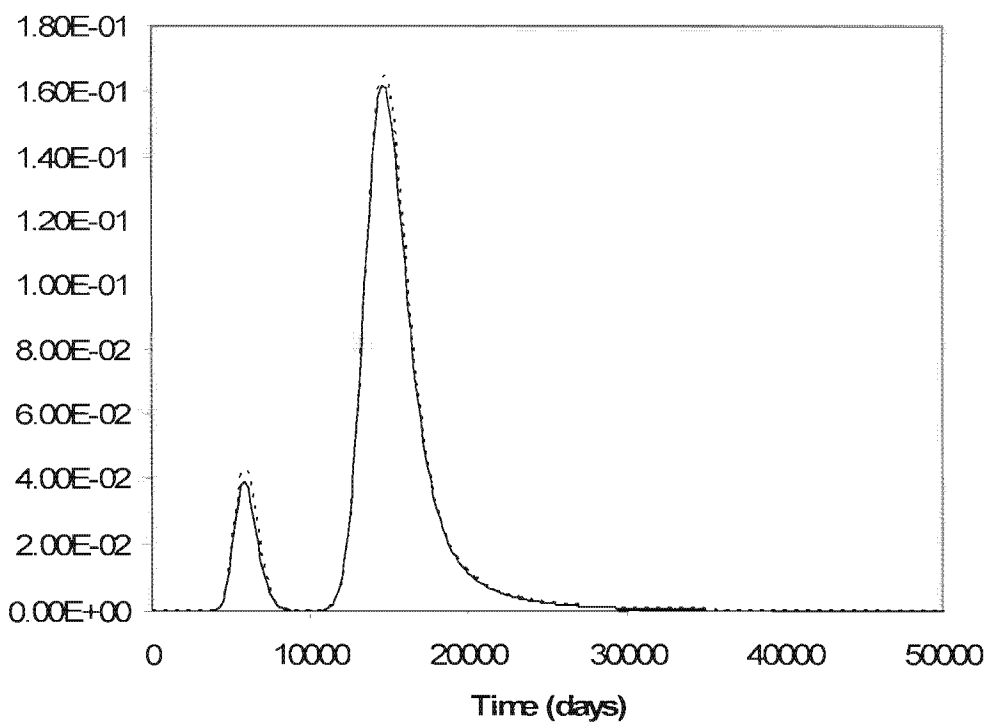
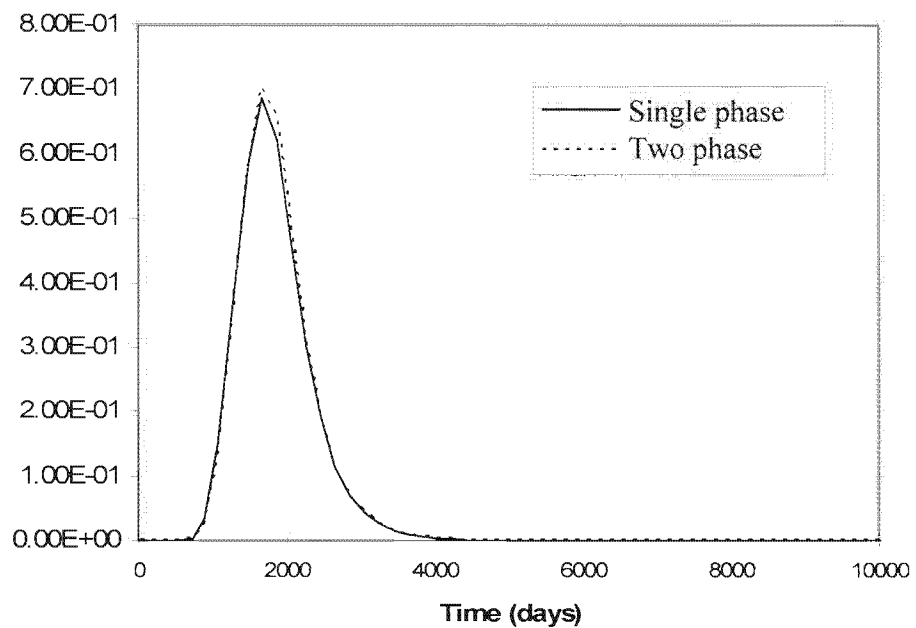
Saturated cell
 Partially-saturated cell

Figure 11 . Results for mixed vadose / saturated zone simulation using single-phase formulation. Open circles show locations for breakthrough curves.



Saturated cell
 Partially-saturated cell

Figure 12. Results for mixed vadose / saturated zone simulation using two-phase formulation. Open circles show locations for breakthrough curves.



Figures 13 and 14 . Concentration breakthrough for the two formulations at observation point a) below the perched layer and b) near the exit point. Locations are indicated in Figure 11.